Biological Forum – An International Journal **16(7): 36-43(2024)**

ISSN No. (Print): 0975-1130
ISSN No. (Online): 2249-3239

Green Synthesis of Nickel Oxide Nanoparticles using Betel Leaf Extract and *Oxalis stricta* Leaf Extract and their Characterization

B. Lavanya[1, 2]*, Y. Aparna[1] and M.V. Ramana[2]
[1]Department of Physics,
Jawaharlal Nehru Technological University, Hyderabad (Telangana), India.
[2]Department of Physics,
Anurag University, Hyderabad (Telangana), India.

(Corresponding author: B. Lavanya)*
(Received: 18 April 2024; Revised: 08 May 2024; Accepted: 03 June 2024; Published: 15 July 2024)
(Published by Research Trend)

ABSTRACT: In the present study, nickel oxide nanoparticles were synthesized using Betel leaf extract and Oxalis stricta leaves. The betel leaf acts as a strong reducing agent and is rich in vitamin C, riboflavin, and a great source of calcium. Oxalis stricta leaves are also rich in vitamin C. Nickel oxide nanoparticles are used for medical applications, including biomedical detection and antibiotics. The synthesized NiO nanoparticles from both plant extracts were examined by X-ray diffraction (XRD), field emission scanning electron microscope (FE-SEM), Fourier transform infrared spectroscopy (FTIR), photoluminescence (PL), and ultraviolet-visible (UV-Vis) spectroscopy. From the results of XRD, the size of the synthesized NiO nanoparticles is calculated using Debye-Scherer formulas and is approximately 12–16 nm in both plant extracts. The FE-SEM confirms that the synthesized NiO nanoparticles are spherical. The FTIR results confirm the formation of NiO nanoparticles with the presence of a Ni-O band in the range of 400 cm^1 to 600 cm^1.

Keywords: Green Synthesis, Betel Leaf, Oxalis Stricta, NiO nanoparticles.

INTRODUCTION

Advancements in various industries and technologies have led to a surge in interest in nanoscale materials, primarily because they possess unique properties that are dependent on size and morphology (Azam *et al.*, 2009; Koparde *et al.*, 2023; Chandra *et al.*, 2019). Nanoparticle synthesis encompasses various techniques, including biological (involving plant parts, bacteria, and fungi), chemical (such as sol-gel, co-precipitation, and hydrothermal), and physical methods (like evaporation-condensation and laser ablation). However, the presence of toxic compounds hampers their practical application and renders them economically unfeasible (Veerasamy *et al.*, 2011). These synthesis routes face challenges due to the necessity of costly metal salts, organic solvents, toxic reducing agents, as well as stabilizing and capping agents (Chandra *et al.*, 2019). Furthermore, these approaches necessitate expensive equipment and pose risks to both the environment and human health (Ramesh & Rajendran 2022). Consequently, researchers have developed eco-friendly methods involving the use of biological systems (known as green synthesis) such as fungi, bacteria, plants, and yeast. Plant extracts, particularly from different parts (leaves, stems, fruits, and flowers), are favored in the preparation of nanoparticles due to their dual role as reducing and capping agents (Iravani *et al.*, 2014; Sagadevan *et al.*, 2023; Berhe & Gebreslassie 2023).

It is established that, during the green synthesis process, phytoconstituents like alkaloids, terpenoids, polyphenols, glycosides, flavonoids, proteins, vitamins, and polysaccharides serve as both capping and reducing agents (Sabouri *et al.*, 2021). Various factors, including the nature and concentration of plant extracts, metal salt, pH, and synthesis protocol, influence the green synthesis of nanoparticles (Hussain *et al.*, 2023). Metal nanoparticles (MNPs) have attracted significant interest from researchers due to their distinct properties, including particle size, shape, crystal structure, surface effects, magnetic, catalytic, and optical properties, as well as chemical and mechanical characteristics differing from their bulk counterparts (Tile *et al.*, 2016; Olajire & Mohammed 2020).

Nickel oxide (NiO) is an inorganic black substance that has a large surface area and a cubic crystalline structure with a band gap ranging from 3.6 eV to 4.0 eV. It exhibits excellent electrochemical performance and also possesses magnetic, mechanical, electronic, and optical properties (Iqbal *et al.*, 2019; Ezhilarasi *et al.*, 2020). Nickel oxide (NiO) is an important transition metal oxide that has gained increasing attention due to its potential use in various applications (Jassim *et al.*, 2023). NiO nanoparticles have demonstrated significant potential in antifungal, antibacterial, antioxidant, anti-

inflammatory, anticancer, and enzyme inhibition activities (Biswas *et al*., 2022). Nickel oxide nanoparticles (NiO NPs) can be obtained through a simple and practical method by heating nickel (II)-based compounds such as hydroxides, nitrates, and carbonates (El-Kemary *et al*., 2013). However, as part of our research, we have explored a green approach for synthesizing NiO NPs using *Piper betle* L. betel leaves (hereafter called BL) and *Oxalis stricta* (hereafter called OSL).

Piper betle L., a perennial creeping plant belonging to the Piperaceae genus, is widely cultivated in India and other tropical Asian countries (Mirzaei & Darroudi 2017; Praburaman *et al.*, 2016). *Piper betle* L. is not only known for its traditional medicinal properties, including its potential to control caries and periodontal disease, reduce inflammation, and exhibit antimicrobial activity, but it has also shown promise in the synthesis of metal nanoparticles (Sharma *et al*., 2015). In recent studies, *Piper betle* L. has been utilized as a reducing and capping agent for various metal nanoparticles due to the presence of organic compounds in its extract (Hafeez *et al*., 2021). The betel plants contain a diverse range of phytochemicals, including chavicol, chavibetol, hydroxychavicol, methyl eugenol, and others. These bioactive compounds are responsible for synthesizing and reducing nanoparticles (Selvanathan *et al*., 2021; Uddin *et al.*, 2021). Shamrock, or Oxalis stricta, is a plant that grows in both full sun and partially shaded conditions and is often heard as a weed in gardens, fields, and lawns. It is rich in vitamin C. The entire plant can be used to prepare herbal tea, and the leaves can be used to make a flavored drink with a lemonade-like flavor. Boiling the whole plant will result in an orange dye. Oxalis stricta leaf extract has been used for treating nausea, pain in the stomach, and fevers.

In this study, we synthesized nickel oxide nanoparticles by using BL and OSL. The present research work reports the synthesis of nickel oxide nanoparticles by using BL extract and OSL extract. The synthesized nanoparticles are characterized using XRD, FESEM, UV-VIS, FTIR, and PL. In addition to this, anti-bacterial and anti-fungal activities are studied for synthesized nanoparticles.

MATERIAL AND METHODS

Nickel Nitrate Hexahydrate ($Ni(NO_3)2.6H_2O$) was purchased from Sigma Aldrich, and fresh betel leaves (BL) were collected from a local farm situated in Bodduppal, Hyderabad, Telangana, India. Fresh leaves of Oxalis stricta leaves (OSL) were collected from Anurag University Campus, Venkatapur, Hyderabad, India.

A. Preparation of plant extract

The collected BL and OSL are washed with distilled water and sun-dried for 15 minutes to get rid of all the dust and unwanted particles. The process was repeated four times. The cleaned 10 gramme leaves of PBL and OSL were cut into fine pieces using a stainless steel blade and transferred into a 250-ml conical flask containing 200 ml of double-distilled water. The mixtures are boiled for 75 minutes at 100ºC using a magnetic stirrer; later, the mixtures are cooled to room temperature. The obtained leaf extract was filtered using Mann filter paper. The collected leaf extracts were stored in a dark glass container for further synthesis of NiO nanoparticles.

B. Synthesis of NiO nanoparticles

5 grams of$Ni(NO_3)_2.6H_2O$ precursor was added to 20 ml of plant extract and heated at 60ºC for 2 hours on a magnetic stirrer resulting in a fine paste. This was washed with distilled water and treated at 100°C for 1 hour, then the resultant was transferred to a furnace, which was maintained at 400°C for 2 hours.

C. Characterization techniques

The synthesized nickel oxide nanoparticles are characterized by an X-ray diffractometer (XRD) (model: X'PERT PRO Analytical), and the diffraction patterns are recorded in the range of 20° to 80°. The surface morphology of nickel oxide nanoparticles is studied by a scanning electron microscope (SEM ZEISS), and their elemental composition is known by EDAX. FTIR is used to identify the bonding and stretching of molecules present in the sample. The transmittance and optical absorption of the nickel oxide NPs were analyzed by using a UV-visible spectrometer. The optical properties of synthesized NiO nanoparticles are studied by photoluminescence emission spectra.

RESULTS AND DISCUSSION

A. X-ray Diffraction (XRD)

The X-ray diffraction pattern of synthesized NiO nanoparticles by using betel leaf extraction and oxalis stricta leaf extraction is shown in Figs. 1 and 2. The diffracted peaks of NiO particles are obtained at 37.28547, 43.33088, 62.92415, 43.33088, 62.92415, 75.46974, 75.46974, and 79.45466 and angles, which correspond to correspond to (111), (200), (220), (311) and (222) planes for betel leaf extract, and 37.27309 and 37.27309, 43.3216, 62.92939,75.48447, and 75.48447, and 79.47602, which correspond to (111), (200), (220), (311) and (222) planes for *Oxalis stricta*. The synthesized nanoparticles are cubic, face-centered, with an average crystallographic size within the range of 12 nm and 15 nm, corresponding to the measured peaks. The size and shape of the nanoparticles and the presence of strain are the main reasons for the observed broadening of the peaks. Scherer's formula is used to calculate the particle size.

$$D = \frac{k\lambda}{\beta\cos\theta} \quad (1)$$

Where D is crystalline size, k is constant, which is equal to 0.9, 2θ is the brags angle, β is the full wave half maximum (FWHM) radians, and λ is the wavelength of X-rays used, *i.e.*, $1.54A^0$.

By using the Brags equation, the interplanar distance d is calculated *i.e.*

$$n\lambda = 2d\sin\theta \quad (2)$$

The synthesized NiO nanoparticles from both plant extracts are found to have a face-centered cubic structure. Hence, the lattice parameter 'a' is calculated by using the formula.

$$a = d\left(\sqrt{(h^2 + k^2 + l^2}\right) \quad (3)$$

The microstrain of a nanoparticle is calculated using a formula.

$$\varepsilon = \frac{\beta}{4\tan\theta} \quad (4)$$

It is observed that the microstrain value decreases with increasing angle θ value.

The length of dislocation lines per unit volume is defined as the dislocation density. Fromthe XRD pattern, the dislocation density is also calculated by the equation

$$\delta = \frac{1}{D^2}$$

Where D is the crystalline size.

The size (D) and microstrain (ε) responses to the XRD peak broadening from the full-width at-half-maximum (FWHM) of the diffraction peaks could be calculated using the Williamson-Hall relation. From the W-H plot, the entire peak broadening can be expressed as the sum of the peak broadening caused by the lattice strain and particle size. It can be written as

$\beta_{hkl} = \beta_D + \beta_s$

Strain-induced broadening is given as Bs = 4ε tan θ. By putting the values of β_D and βs in the above equation, we get

$$\beta_{hkl} = \frac{k\lambda}{D} + 4\varepsilon \sin\theta \quad (5)$$

The above equation is in the form of a straight line equation, *i.e.*, y = mx + c, where $\frac{k\lambda}{D}$ is an intercept made by a straight line and ε is the strain, which represents the slope of the line. A graph is plotted between 4 sin θ and β Cos θ, which givesthestrain present in the sample.

Hence, the sizes of NiOnanoparticles obtained from W-H analysis are well correlated with the sizes estimated using Scherrer's formula.

From the XRD and W-H plots of the synthesized NiO nanoparticles, sizes are compared, and strain values are calculated. All the values obtained from XRD data and the W-H graph are tabulated in Table 1.

From the XRD results, it is observed that no other different diffraction peaks are present in the XRD pattern, which indicates that other crystal products are not retained in the sample, and the sharp peaks show that the nanoparticles are well crystallized. The interplanar distance, lattice parameter, particle size, and microstrain values are calculated and tabulated in Table 1.

From the W-H plot, the particle size is calculated for both plant extracts, which are about 11.58 nm and 14.2 nm. The microstrain is calculated for both plant extracts, and it is observed that for betel leaf extract, the slope value is positive, and for oxalis stricta leaf extract, the slope value is negative, which indicates lattice expansion and lattice compression in the synthesized NiO nanoparticles. The strain values obtained from the W-H plot are tabulated in Table 1.

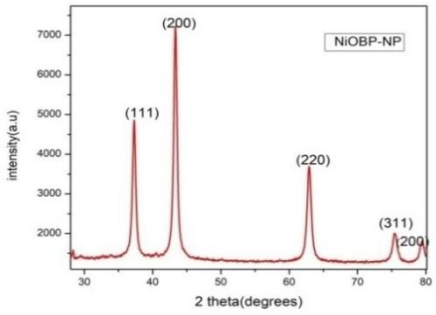

Fig. 1.

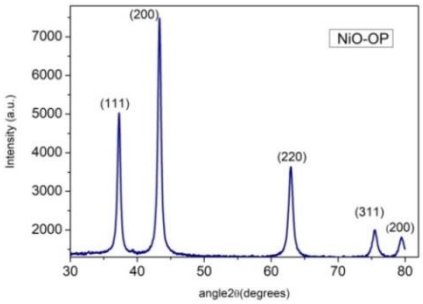

Fig. 2.

Fig. 1, 2 represent the XRD patterns of synthesized NiO nanoparticles from BL extract and OS leaf extract

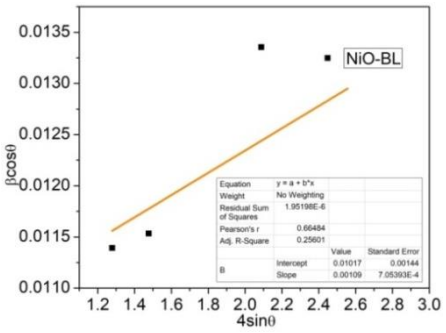

Fig. 3.

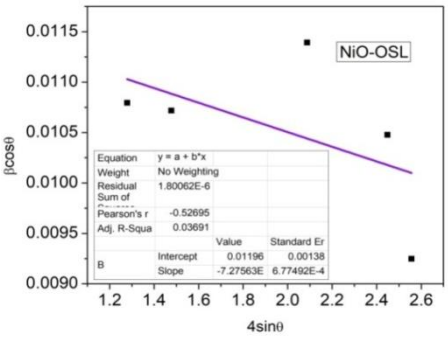

Fig. 4.

Figs. 3, 4 represent the W-H plot for synthesized NiO nanoparticles from BL extract and OSL extracts.

B. Field Emission Scanning electron microscope (SEM)

Figs. 5, 6 show the images of synthesized NiO nanoparticles from the BL extract and OSL extract. From the SEM image, the morphology of the synthesized nanoparticles was observed to be in spherical and cubical shapes for both plant extracts. The size of the nanoparticles is calculated using Imagej software, which ranges from 11 nm to 36 nm in size for both plant extracts.

The average particle size observed from the SEM analysis is 20.23 nm and 27 nm for BL extract and OSL extract, which are a little bit larger than the nanoparticle size predicted from the XRD analysis. The sizes of nanoparticles in SEM are comparable to those in previous literature (Rahdar *et al*., 2015).

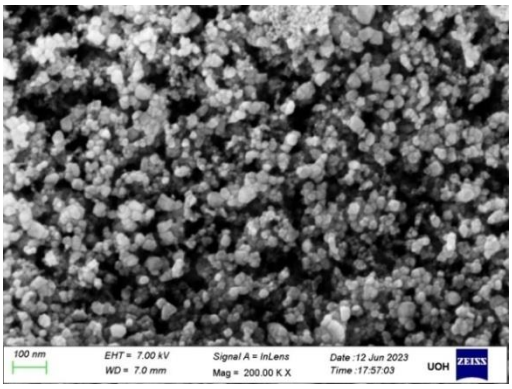

Fig. 5.

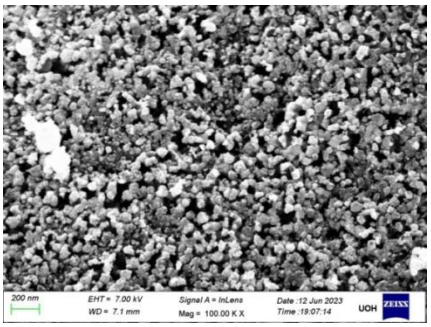

Fig. 6.

Figs. 5, 6 represent the SEM images of samples of NiO nanoparticles synthesized from OSL and BL extracts.

C. Energy Dispersive X-ray (EDX)

Figs. 7, 8 show the EDX concentration of elements present in the synthesized NiO nanoparticles from Betel and Oxalis stricta leaf extract.

The EDX is carried out by using energy dispersive-ray spectroscopy measurements. In the EDX spectrum of NiO nanoparticles, the peaks correspond to Ni and O elements. No additional impurities or non-existent carbon are contained in the sample. Ni ratios in both samples are almost equal, and the atomic percentage is the same.

Table 1: Gives the values of Crystallite size, strain, and Dislocation density from XRD and W-H.

Sample	θ(RADIANS)	HWFM(β) RADIANS	D=(Kλ/(βcosθ))	Size odtained by WH plot	d=nλ/2sinθ	a=d*√(h²) +k²+l²	micro strain= β/4tan theta θ	strain from wH plot	Dislocation density=1/d²
Betal leaf extract	0.325377107	0.0056789	12.83904125		0.240876317	0.416716029	0.008442557		0.006066453
	0.378133262	0.0065997	12.93086019		0.208566814	0.417133628	0.007258223		0.005980606
	0.549116798	0.0095839	12.16627797	14.2 nm	0.147528211	0.41720978	0.005456697	7.2756×10^{-4}	0.00675592
	0.658597724	0.0114947	13.2286331		0.125815254	0.41727887	0.004279873		0.005714392
	0.693372712	0.0121016	14.98538378		0.120475378	0.417338755	0.003617787		0.004453119
Oxalis Stricta	0.325269071	0.0113883	12.8438859		0.24095348	0.41684952	0.008442076		0.006061877
	0.378052279	0.0117878	12.65130794	11.58nm	0.208609342	0.417218683	0.007420118		0.006247829
	0.549162526	0.0150669	10.7847368		0.147517187	0.417178604	0.006155248	-9.735×10^{-4}	0.008597673
	0.658726268	0.0158287	11.07300013		0.125794359	0.417209573	0.005112206		0.008155853
	0.693559113	0.0146749	12.28217891		0.120448363	0.417245173	0.004413041		0.006629017

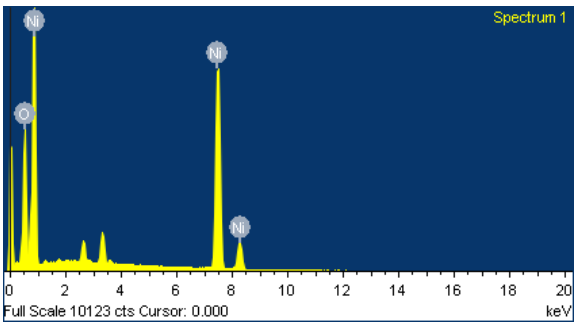

Fig. 7.

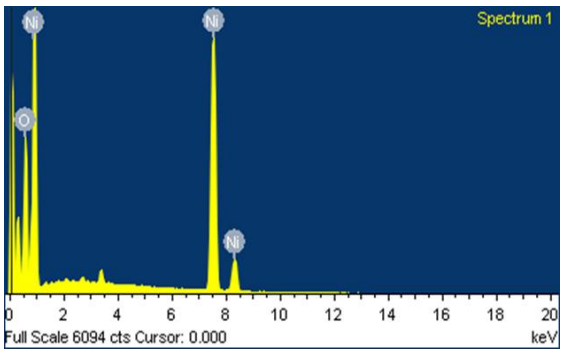

Fig. 8.

Figs. 7, 8 EDAX of NiO nanoparticles synthesized from BL extract and OSL extract

Table 2.

Element	Weight %	Atomic%
O K	22.95	50.79
Ni K	77.05	49.21
Totals	100.00	

Table 3.

Element	Weight %	Atomic %
O K	21.95	50.79
Ni K	78.05	49.21
Totals	100.00	

Table 2, 3 represent the weight percent and atomic percent of Ni and O atoms.

D. Fourier transform infrared spectroscopy (FTIR)

The FTIR spectroscopy of synthesized nanoparticles confirms the formation of NiO particles. In FTIR, from the stretching and binding modes of vibration, the presence of a molecule can be identified. The radiation is allowed on the samples in the range of 300 cm^1 to 2500 cm^1 for both samples. It is observed that from the FTIR, the peaks formed in the range of 400–600 cm^1 (Dejam *et al*., 2023) confirm the presence of NiO staining in both leaf extracts. The peak around 2003 cm^1 was assigned to O=C=O (Balakrishnan *et al*., 2023) symmetric and asymmetric stretching vibrations in Betal leaf extract. The board absorption of around 779 cm^1 is due to C=O stretching vibrations. The peak at 606 cm^1 is assigned to the Ni-O-H stretching bond in betel leaf extract. Whereas in Oxalis stricta leat extract, noother peakes were observed.

Table 4: FTIR Spectra analysis.

Molecule bonding	Frequency(cm^{-1})
NiO strecthing	400 cm^{-1}- 600 cm^{-1}
Ni-O-H strecthing bond	606 cm^{-1}
C=O	779 cm^{-1}
O=C=O	2003 cm^{-1}

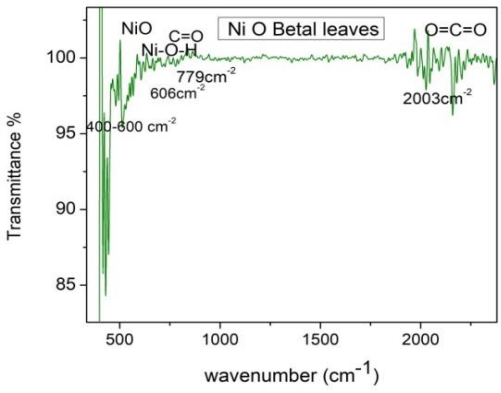

Fig. 9.

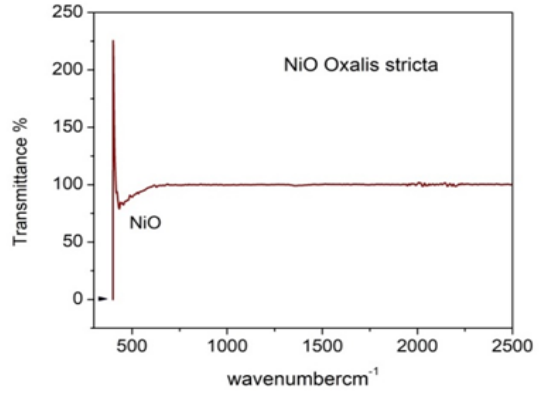

Fig. 10.

Figs. 9, 10 represent the FTIR for synthesized NiO nanoparticles for BL extract and OSL extract.

E. UV-Visible Spectroscopy (UV-Vis)

The UV-Vis absorption spectra are shown in Figs. 9-11 for synthesized NiO nanoparticles from BL extract and OSL leaf extract. The UV-Vis optical properties are studied, and the band gap is calculated. The absorption spectra of synthesized nanoparticles are recorded from the wavelength of 200 nm to 800 nm. In both spectra, the blue shift is observed for shorter wavelengths, which is due to quantum confinement effects, which can be attributed to a decrease in the size of nanoparticles (Barve *et al.*, 2021). The absorption bands are observed at 217 nm and 240 nm for Betal and Oxalis leaf extracts. The energy gap of synthesized NiO nanoparticles from both extracts was calculated using the Tauc equation.

i.e., $\alpha h\nu = A(h\nu - Eg)^n$, where α is the absorption coefficient, A is absorbance, $h\nu$ is the photon energy, Eg is the energy gap, and n is the nature of the transition path. Here n=1/2, as in this direct transition. A graph is plotted between $(\alpha h\nu)2$ verses $h\nu$ for synthesized NiO nanoparticles, and a straight line is extrapolated onto the X-axis, which gives the energy gap of the NiO nanoparticles from both plant extracts, as shown in Fig. From the graph, it is observed that the 3.54 eV and 3.35 eV are for betel and Oxalis stricta leaf extracts, respectively.

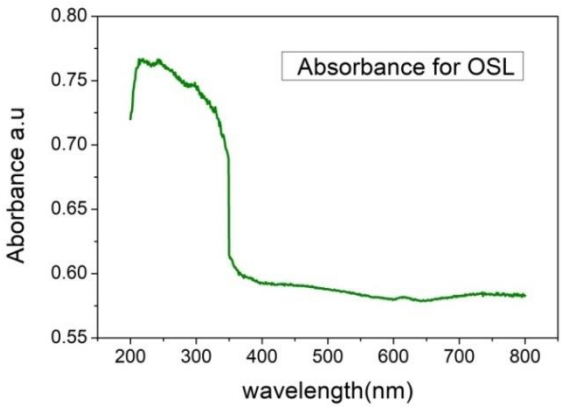

Fig. 11.

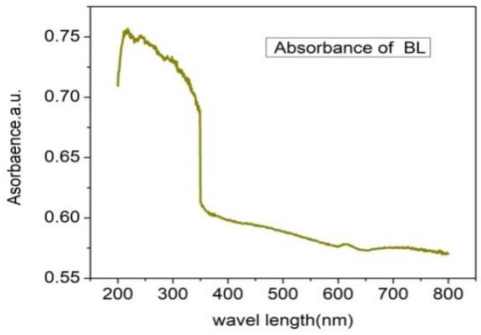

Fig. 12.

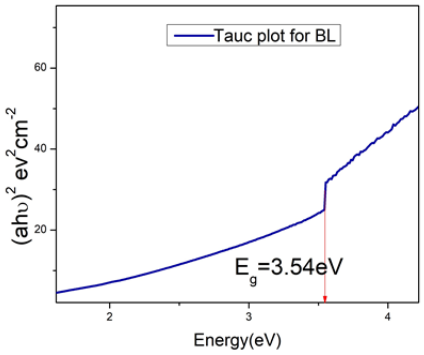

Fig. 13.

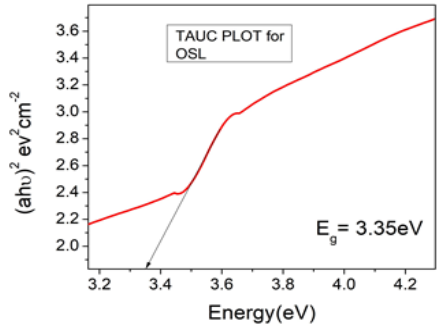

Fig. 14.

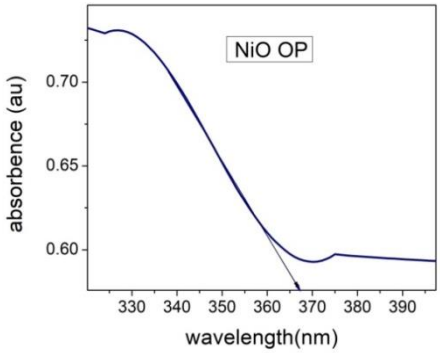

Fig. 15.

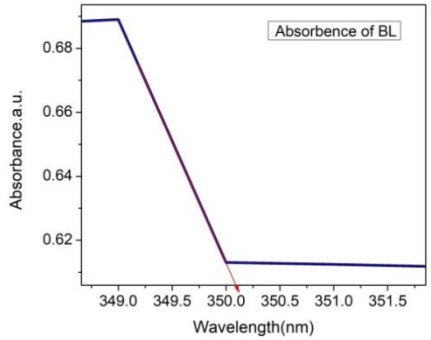

Fig. 16.

Figs-13, 14 represent the Tauc plot for BL extract and OSL extract.

Figs-11, 12, 15,16 represent the UV-Vis spectrum for BL extract and OSL extract.

F. Photoluminescence

Photoluminescence is used to study the efficiency of the emitted light of metal oxide-synthesized nanoparticles. PL intensity can be in good agreement with the defect density in metal oxides. It is also used to identify the structural defects, *i.e.*, cationic and anionic vacancies, charge excitation, and electron structure of nanoparticles. The near-band edge of UV emission and the deep-level defect to visible emission are the two categories of PL emission. The direct recombination of excitons via exciton-exciton scattering is observed in UV emission, and the recombination of a photo-generated hole with an electron occupying the oxygen vacancy is in visible emission.

The photo-luminescence emission spectrum of synthesized NiO nanoparticles is recorded in the wavelength range of 350 nm to 600 nm for Betal and Oxalis stricta leaf extract, as shown in Fig. 7. The emission spectra are recorded with an excitation wavelength of 320 nm at room temperature for both leaf extracts.

For the synthesized NiO nanoparticles in the PL spectra, the peaks are observed at 358 nm, 446 nm, 469 nm, 537 nm, and 559 nm for the beta leaf extract and 377 nm, 448 nm, 495 nm, 537 nm, and 569 nm for the Oxalis stricta leaf extract. The peaks at 358 nm and 377 nm are related to the UV spectrum. The peak at 446 nm and 448 nm corresponds to the violet luminescence, and it is due to the possible transition of trapped electrons of Ni to the valance band. The blue luminescence is observed at 469 nm and 495 nm peaks, which appear through the recombination of electrons from the nickel vacancy to the holes in the valance band. The green luminescence that is observed at 537 nm, 559 nm, and 569 nm is attributed to nickel vacancies. NiO nanoparticles show effective green band emission, so they are used in optoelectronic nanodevices.

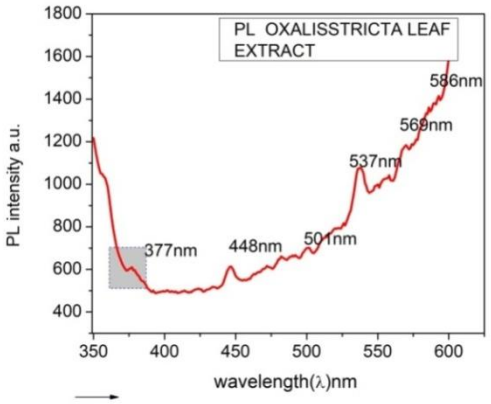

Fig. 17.

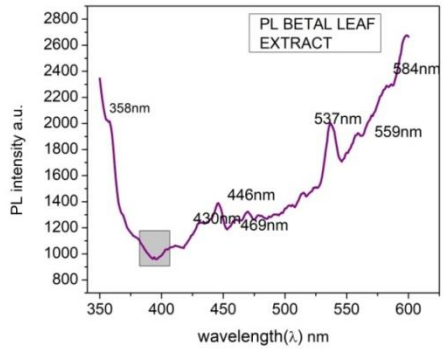

Fig. 18.

Figs. 17, 18 represent the PL emission spectra for BL extract and OSL extract.

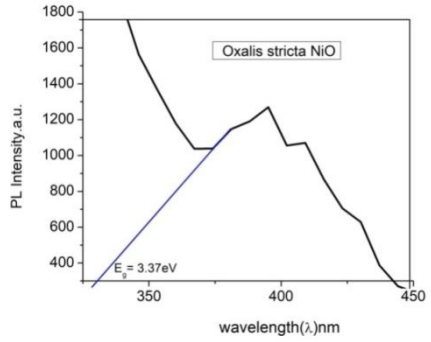

Fig. 19.

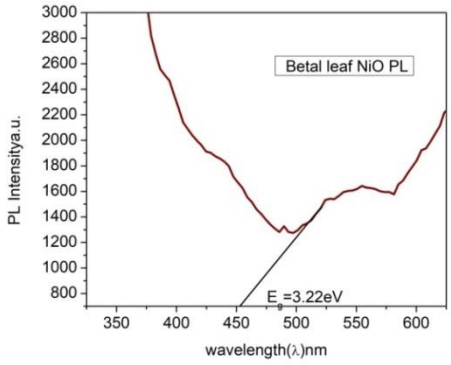

Fig. 20.

Figs. 19, 20 represent the determination of band gap from PL spectra for BL extract and OSL extract.

CONCLUSIONS

In the present work, the NiO nanoparticles were synthesized by the green method (novel, non-toxic, and cheap) using Betel leaf (BL) extract and Oxalis stricta leaf (OSL) extract. The average crystallite size from XRD and crystallite size from the W-H plot for BL extract is 13.22 nm and 14.2 nm, and for OSL extract, it is 11.91 nm and 11.58 nm. From this, it is observed that the crystallite size is almost equal. The XRD shows that the synthesized NiO nanoparticles possess a face-centered cubic structure. From the results of FESEM, the synthesized nanoparticles are spherical, and the particle size estimated from FESEM is about 11 nm to 36 nm for both plant extracts. From EDAX, it is confirmed that the synthesized nanoparticle has only Ni and O elements, and the non-existence of carbon is shown in EDAX. The functional groups of NiO were confirmed by FTIR, which exists between 400 cm^1 and 600 cm^1 for BL and OSL extracts. From UV-Vis, it is confirmed that the synthesized NiO nanoparticles are direct band semiconductors, and the band gap is calculated, which is obtained as 3.54 eV and 3.55 eV for BL and OSL extracts. From photoluminescence, the green absorption band is observed at 537 nm (2.30 eV). The other emission peaks show the structural defects formed in synthesized NiO nanoparticles for BL and OSL extracts.

FUTURE SCOPE

To Synthesise metal Oxide nanoparticles at low cost, and eco-friendly. And to use on a large scale for industrial purposes.

Acknowledgement. The authors are thankful to Anurag University and Hyderabad Central University (HCU) for synthesizing and characterization techniques.One of the Author(B. L) would like to thank Head of the Department of Physics, AnuragUniversity, Hyderabad for his encouragement and support.
Conflict of Interest. None.

REFERENCES

Azam, A., Ahmed, F., Arshi, N., Chaman, M., & Naqvi, A. H. (2009). One step synthesis and characterization of gold nanoparticles and their antibacterial activities against E. coli (ATCC 25922 strain). *International Journal of Theoretical and Applied Sciences*, *1*(2), 1–4.

Barve, A. K., Gadegone, S. M. & Lanjewar, R. B. (2021). Synthesis and Morphological Study of Nickel Oxide Nanoparticle. *International Journal of Advanced Research in Science, Communication and Technology*, 1–5.

Balakrishnan, K., Thangavel, G., & Murugesan, N. (2023). Structural, morphological, optical and electrochemical. In *Int. J. Nano Dimens* (Vol. 14, Issue 2).

Berhe, M. G., & Gebreslassie, Y. T. (2023). Biomedical Applications of Biosynthesized Nickel Oxide Nanoparticles. In *International Journal of Nanomedicine* (Vol. 18, pp. 4229–4251). Dove Medical Press Ltd.

Biswas, P., Anand, U., Saha, S. C., Kant, N., Mishra, T., Masih, H., Bar, A., Pandey, D. K., Jha, N. K., Majumder, M., Das, N., Gadekar, V. S., Shekhawat, M. S., Kumar, M., Radha, Proćków, J., Lastra, J. M. P. de la, & Dey, A. (2022). Betelvine (*Piper betle* L.): A comprehensive insight into its ethnopharmacology, phytochemistry, and pharmacological, biomedical and therapeutic [1] P. Biswas "Betelvine (*Piper betle* L.): A comprehensive insight into its ethnopharmacology, phytoche. In *Journal of Cellular and Molecular Medicine*, *26*(11), 3083–3119. John Wiley and Sons Inc.

Chandra, H., Patel, D., Kumari, P., Jangwan, J. S., & Yadav, S. (2019). Phyto-mediated synthesis of zinc oxide nanoparticles of Berberis aristata: Characterization, antioxidant activity and antibacterial activity with special reference to urinary tract pathogens. *Materials Science and Engineering C*, *102*, 212–220.

Dejam, L., Sabbaghzadeh, J., Ghaderi, A., Solaymani, S., Matos, R. S., Tălu, Stefan, da Fonseca Filho, H. D., Sari, A. H., Kiani, H., Shayegan, A. H. S., & Doudaran, M. A. (2023). Advanced nano-texture, optical bandgap, and Urbach energy analysis of NiO/Si heterojunctions. *Scientific Reports*, *13*(1).

El-Kemary, M., Nagy, N., & El-Mehasseb, I. (2013). Nickel oxide nanoparticles: Synthesis and spectral studies of interactions with glucose. *Materials Science in Semiconductor Processing*, *16*(6), 1747–1752.

Ezhilarasi, A. A., Vijaya, J. J., Kaviyarasu, K., Zhang, X., &Kennedy, L. J. (2020). Green synthesis of nickel oxide nanoparticles using Solanum trilobatum extract for cytotoxicity, antibacterial and photocatalytic studies. *Surfaces and Interfaces*, *20*.

Hafeez, M., Shaheen, R., Akram, B., Ahmed, M. N., Zain-Ul-Abdin, Haq, S., Din, S. U., Zeb, M., & Khan, M. A. (2021). Green Synthesis of Nickel Oxide Nanoparticles using Populus ciliata Leaves Extract and their Potential Antibacterial Applications. *South African Journal of Chemistry*, *75*.

Hussain, S., Ali Muazzam, M., Ahmed, M., Ahmad, M., Mustafa, Z., Murtaza, S., Ali, J., Ibrar, M., Shahid, M., & Imran, M. (2023). Green synthesis of nickel oxide nanoparticles using *Acacia nilotica* leaf extracts and investigation of their electrochemical and biological properties. *Journal of Taibah University for Science*, *17*(1).

Iravani, S., Korbekandi, H., Mirmohammadi, S. V. and Zolfaghari, B. (2014). Synthesis of silver nanoparticles: chemical, physical and biological methods. In Research in Pharmaceutical Sciences (Vol. 9)

Iqbal, J., Abbasi, B. A., Mahmood, T., Hameed, S., Munir, A., & Kanwal, S. (2019). Green synthesis and characterizations of Nickel oxide nanoparticles using leaf extract of Rhamnus virgata and their potential biological applications. *Applied Organometallic Chemistry*, *33*(8).

Jassim, S. M., Abd, M. A., & Hammed, I. A. (2023). Green synthesis of Nickel Oxide Nanoparticles using Syzygium Aromatic Extract: Characterization and Biological Applications. *Al-Bahir Journal for Engineering and Pure Sciences*, *2*(2).

Koparde, A., Shete, A., Patil, A., Mali, D., Durgawale, T., Yeligar, V. C., Shewale, M., Kadam, A. and Jadhav, R. (2023). Preparation and characterization of silver nanoparticles using Cissus quadrangular is extract and its in vitro anti-arthritic activity. *Biological Forum-An International Journal*, *15*(3), 665-668.

Mirzaei, H., & Darroudi, M. (2017). Zinc oxide nanoparticles: Biological synthesis and biomedical applications. *Ceramics International*, *43*(1), 907–914.

Olajire, A. A., & Mohammed, A. A. (2020). Green synthesis of nickel oxide nanoparticles and studies of their photocatalytic activity in degradation of polyethylene films. *Advanced Powder Technology*, *31*(1), 211–218.

Praburaman, L., Jang, J. S., Muthusamy, G., Arumugam, S., Manoharan, K., Cho, K. M., Min, C., Kamala-Kannan, S., & Byung-Taek, O. (2016). Piper betle-mediated synthesis, characterization, antibacterial and rat splenocyte cytotoxic effects of copper oxide nanoparticles. *Artificial Cells, Nanomedicine and Biotechnology*, *44*(6), 1400–1405.

Rahdar, A., Aliahmad, M., & Azizi, Y. (2015). NiO Nanoparticles: Synthesis and Characterization. In *JNS*(Vol. 5).

Ramesh, P., & Rajendran, A. (2022). Green synthesis of nickel oxide nanoparticles for photodegradation analysis. *Materials Today: Proceedings*, *68*, 367–372.

Sabouri, Z., Rangrazi, A., Amiri, M. S., Khatami, M., & Darroudi, M. (2021). Green synthesis of nickel oxide nanoparticles using *Salvia hispanica* L. (chia) seeds extract and studies of their photocatalytic activity and cytotoxicity effects. *Bioprocess and Biosystems Engineering*, *44*(11), 2407–2415.

Sagadevan, S., Fatimah, I., Anita Lett, J., Rahman, M. Z., Leonard, E., & Oh, W. C. (2023). Eco-friendly green approach of nickel oxide nanoparticles for biomedical applications. In *Open Chemistry* (Vol. 21, Issue 1). Walter de Gruyter GmbH.

Selvanathan, V., Shahinuzzaman, M., Selvanathan, S., Sarkar, D. K., Algethami, N., Alkhammash, H. I., Anuar, F. H., Zainuddin, Z., Aminuzzaman, M., Abdullah, H., & Akhtaruzzaman, M. (2021). Phytochemical-assisted green synthesis of nickel oxide nanoparticles for application as electrocatalysts in oxygen evolution reaction. *Catalysts*, *11*(12).

Sharma, A. K., Desnavi, S., Dixit, C., Varshney, U., & Sharma, A. (2015). Extraction of Nickel Nanoparticles from Electroplating Waste and Their Application in Production of Bio-diesel from Biowaste. *International Journal of Chemical Engineering and Applications*, *6*(3), 156–159.

Tile, V. G., Suraj, H., Uday, B., & Sahana, S. (2016). Recent Trends in Nanotechnology and its Future Scope-A Review. *International Journal on Emerging Technologies (Special Issue on ICRIET-2016)*, *7*(2), 377–385.

Uddin, S., Safdar, L. Bin, Anwar, S., Iqbal, J., Laila, S., Abbasi, B. A., Saif, M. S., Ali, M., Rehman, A., Basit, A., Wang, Y., & Quraishi, U. M. (2021). Green synthesis of nickel oxide nanoparticles from berberis balochistanica stem for investigating bioactivities. *Molecules*, *26*(6).

Veerasamy, R., Xin, T. Z., Gunasagaran, S., Xiang, T. F. W., Yang, E. F. C., Jeyakumar, N., & Dhanaraj, S. A. (2011). Biosynthesis of silver nanoparticles using mangosteen leaf extract and evaluation of their antimicrobial activities. *Journal of Saudi Chemical Society*, *15*(2), 113–120.

How to cite this article: B. Lavanya, Y. Aparna and M.V. Ramana (2024). Green Synthesis of Nickel Oxide Nanoparticles using Betel Leaf Extract and *Oxalis stricta* Leaf Extract and their Characterization. *Biological Forum – An International Journal, 16*(7): 36-43.